

---

# Identifying Causal Structure in Dynamical Systems

---

Dominik Baumann<sup>1,2</sup>, Friedrich Solowjow<sup>1</sup>, Karl H. Johansson<sup>2</sup>,  
and Sebastian Trimpe<sup>1,3</sup>

<sup>1</sup>: Max Planck Institute for Intelligent Systems, Stuttgart, Germany

<sup>2</sup>: Division of Decision and Control Systems, KTH Stockholm, Sweden

<sup>3</sup>: Data Science in Mechanical Engineering, RWTH Aachen University, Germany

## Abstract

We present a method for automatically identifying the causal structure of a dynamical control system. Through a suitable experiment design and subsequent causal analysis, the method reveals, which state and input variables of the system have a causal influence on each other. The experiment design builds on the concept of controllability, which provides a systematic way to compute input trajectories that steer the system to specific regions in its state space. For the causal analysis, we leverage powerful techniques from causal inference and extend them to control systems. Further, we derive conditions that guarantee discovery of the true causal structure of the system and show that the obtained knowledge of the causal structure reduces the complexity of model learning and yields improved generalization capabilities. Experiments on a robot arm demonstrate reliable causal identification from real-world data and extrapolation to regions outside the training domain.

## 1 Introduction

Modern control systems, such as mobile robots, are envisioned to autonomously act in the real world and to interact with their environment. Since not all situations they may encounter can be foreseen at design time, these systems need to be able to generalize and to transfer obtained knowledge to new problem settings. However, such capabilities are a particular weakness of current machine learning methods [41]. One reason for this is that most machine learning methods only learn correlations. Correlation-based analyses will typically find spurious correlations, which can lead to catastrophic errors when extrapolating outside the training data. Causal learning is seen as a building block towards realizing systems that can adapt and generalize to new tasks [34].

To define causality, mainly two notions are of practical relevance [13]. The first is *temporal precedence*: causes precede their effects. This is also what is understood as causality in systems theory [18, p. 31]. However, here, we mainly focus on the second notion, *physical influence*: manipulating causes changes the effects. In other words, we seek experimental routines and tests that enable control systems to learn, (i) what is the influence of their internal states on one another, and (ii) which of their inputs influence which internal states.

In causal inference, much work has been devoted to inferring causal structure from given data [29]. For control systems, solely relying on given data is not necessary. Such systems are equipped with an input, which they can use to actively conduct experiments for causal inference. Causal inference from experiments, or interventions, has also been studied, most prominently in the context of the do-calculus [33]. However, there it is assumed that state variables can be directly influenced by the input, which is often not possible in control systems. Different from those works, we consider a notion of *controllability*, i.e., how the system can be steered to particular regions in the state space through appropriate input trajectories. Causal relations between variables of a control system should become visible in the mathematical model describing its dynamics. Obtaining such models has

extensively been studied in system identification [22, 42] and in model learning [30]. However, those methods typically use correlation-based analyses to fit a model to data, which unfortunately forces them to usually find spurious correlation. A causal analysis can reveal such spurious correlations and remove corresponding model parameters, thus reducing the parameter space and enhancing the generalization capabilities of the model. In this work, we propose to combine experiment design via the notion of controllability with causal analysis. Combining these powerful concepts from systems theory and causal learning, we obtain a method that identifies the causal structure of control systems and thus improves generalization capabilities and reduces computational complexity.

**Contributions.** We present an algorithm that identifies a dynamical control system’s causal structure through an experiment design based on a suitable controllability notion and a subsequent causal analysis. For the causal analysis, we leverage powerful kernel-based statistical tests based on the maximum mean discrepancy (MMD) [17]. Since the MMD has been developed for independent and identically distributed (i.i.d.) data, we extend it by deriving conditions under which the MMD still yields valid results and by coming up with a test statistic for hypothesis testing, despite non-i.i.d. data. In terms of controllability, we investigate three different settings: *(i)* exact controllability, where we can exactly steer the system to a desired position, *(ii)* stochastic controllability, where we can only steer the system to an  $\epsilon$ -region around the desired position, and *(iii)* the special case of linear systems with Gaussian noise that are controllable in the sense of Kalman. We demonstrate the applicability of the proposed method by automatically identifying the causal structure of a robotic system. Further, for this system, we show improved generalization capabilities inherited through the causal identification.

## 2 Related Work

This paper presents a novel technique for automatically identifying the causal structure of a dynamical system based on MMD statistical tests. In this section, we relate the contribution to the literature.

**Causal inference for dynamical systems.** Causal inference in dynamical systems or time series has been studied in [11, 12, 27, 24] using vector autoregression, in [36] based on structural equation models, in [14], using the fast causal inference algorithm [49] and in [8] and [38], applying kernel mean embeddings and directed information, respectively. None of the mentioned references investigates experiment design. Instead, they aim at inferring the causal structure from given data.

**Experiment design.** A well-known concept for causal inference from experiments is the do-calculus. In the basic setting, a variable is clamped to a fixed value, and the distribution of the other variables conditioned on this intervention is studied [33]. Extensions to more general classes of interventions exist, see, e.g., [56, 46], but they consider static models, which is different from the dynamical systems studied herein. Causal inference in dynamical systems or time series with interventions has been investigated in [13, 35, 28, 40, 48]. However, therein it is assumed that one can directly manipulate the variables, e.g., by setting them to fixed values or forcing them to follow a trajectory. None of those works considers various degrees of controllability, which is the case in this paper.

**Model selection.** An alternative to directly testing causal relations between variables is to choose between a set of candidate models. Such algorithms have been developed in system identification. Well-known examples are the Akaike information criterion [2] and the Bayesian information criterion [43]. In neuroimaging, there are dynamic causal models [15, 52]. In both cases, the methods can only find the true causal structure if such a model is part of the set of candidate models.

**Structure detection in dynamical systems.** Revealing causal relations in a dynamical system can be interpreted as identifying its structure. Related ideas exist in the identification of hybrid and piecewise affine systems [39, 20]. These approaches try to find a trade-off between model complexity and fit, but cannot guarantee to find the true causal structure. Further methods that identify structural properties of dynamical systems can be found in topology identification [25, 45, 54] and complex dynamic networks [5, 21, 57]. Those works seek to find interconnections between subsystems instead of identifying the inner structure of a system as done herein. Moreover, while the mentioned works often rely on restrictive assumptions such as known interconnections or linear dynamics, our approach can deal with nonlinear systems and does not require prior knowledge.

**Kernel mean embeddings.** For causal inference, we will leverage concepts based on kernel mean embeddings, which have been widely used for causal inference [37, 7, 23]. A downside of those

methods is that they typically assume that data has been drawn i.i.d. from the underlying probability distributions. Extensions to non-i.i.d. data exist [9, 10], but rely on mixing time arguments. Dynamical systems, as investigated in this work, often have large mixing times or do not mix at all [47]. Therefore, these types of analyses are not sufficient in this case.

### 3 Problem Setting and Main Idea

We consider dynamical control systems of the form

$$x(t) = f(x(0), u(0:t), v(0:t)) \quad (1)$$

with discrete time index  $t \in \mathbb{N}$ , state  $x(t) \in \mathcal{X} \subset \mathbb{R}^n$ , state space  $\mathcal{X}$ , input  $u(t) \in \mathcal{U} \subset \mathbb{R}^m$ , input space  $\mathcal{U}$ , and  $v(t) \in \mathbb{R}^n$  an independent random variable sequence. The notation  $(0:t)$  here denotes the whole trajectory from 0 to  $t$ . In the following, we will omit this notation and simply write  $u$  or  $v$  if we consider the whole trajectory. The description of the system in (1) is different from the standard, incremental version  $x(t+1) = \tilde{f}(x(t), u(t), v(t))$ . Specifically, (1) emphasizes the dependence of  $x$  at time  $t$  on the initial state. Equation (1) can be obtained from  $\tilde{f}$ . Based on (1), we define non-causality for state and input components by adapting the definition given in [55]:

**Definition 1** (Global non-causality). *The state variable  $x_j$  does not cause  $x_i$  if  $x_i(t) = f_i(x_{1,\dots,n \setminus j}(0), x_j^I(0), u, v) = f_i(x_{1,\dots,n \setminus j}(0), x_j^{II}(0), u, v)$  for all  $x_j^I(0), x_j^{II}(0)$ . Similarly,  $u_j$  does not cause  $x_i$  if  $x_i(t) = f_i(x(0), u_{1,\dots,m \setminus j}^I, v) = f_i(x(0), u_{1,\dots,m \setminus j}^{II}, v)$  for all  $u_j^I, u_j^{II}$ .*

For causal inference, we will exploit that we can influence (1) through  $u$ . To make the notion of *how* we can influence the system precise, we adopt controllability definitions for stochastic systems [53, 4]:

**Definition 2.** *The system (1) is said to be completely  $\epsilon$ -controllable in probability  $\eta$  in the normed square sense in the time interval  $[0, t_f]$  if for all desired states  $x_{\text{des}}$  and initial states  $x(0)$  from  $\mathcal{X}$ , there exists an input sequence  $u$  from  $\mathcal{U}$  such that  $\Pr\{\|x(t_f) - x_{\text{des}}\|_2^2 \geq \epsilon\} \leq 1 - \eta$ , with  $0 < \eta < 1$ .*

A variety of methods exist to identify or learn models for systems (1), e.g., Gaussian process regression or fitting linear state space models using least squares. In the following, we assume that we can obtain an estimate  $\hat{f}$  of the investigated system (1) (including an estimate of the distribution of  $v(t)$ ) using correlation-based analyses. Which method is used is irrelevant for the developed causal identification procedure. This model estimate  $\hat{f}$ , obtained without further assumptions or physical insights, will almost surely entail spurious correlation and suggest causal influences that are actually not present in the physical system. But it will allow us to (approximately) steer the system to specific initial conditions and start experiments from there.

We propose two types of experiments to test for causal relations. For the first type, we investigate whether  $x_j$  causes  $x_i$ . We conduct two experiments (denoted by I and II) with different initial conditions  $x_j^I(0) \neq x_j^{II}(0)$ , while all others are kept the same (cf. Fig. 1). This can be formalized as:

$$x_\ell^I(0) = x_\ell^{II}(0) \forall \ell \neq j, \quad x_j^I(0) \neq x_j^{II}(0) \quad u_\ell^I(t) = u_\ell^{II}(t) \forall \ell, t. \quad (2a)$$

By comparing the resulting trajectories of  $x_i^I$  and  $x_i^{II}$  we can then check whether the change in  $x_j(0)$  caused a different behavior. For checking the similarity of trajectories, we will use the MMD, whose mathematical definition we provide in the next section. The second type of experiments is analogous to the first, but instead of varying initial conditions, we consider different input trajectories  $u_j^I \neq u_j^{II}$ ,

$$x_\ell^I(0) = x_\ell^{II}(0) \forall \ell \quad u_\ell^I(t) = u_\ell^{II}(t) \forall \ell \neq j, t, \quad u_j^I(t) \neq u_j^{II}(t) \forall t. \quad (2b)$$

In the remainder, we address the following problems: (i) we derive conditions that guarantee a valid test and present an approach for obtaining a test statistic for the MMD despite non-i.i.d. data; (ii) we make the experiment design precise and incorporate the fact that we cannot exactly steer the system to specific initial conditions; (iii) we demonstrate the applicability of the method on a robotic system.

### 4 Causal Identification for Dynamical Systems

We will now develop the causality testing procedure. First, we introduce the MMD [17], which we shall use as a measure of similarity. The MMD can be used to check whether two probability

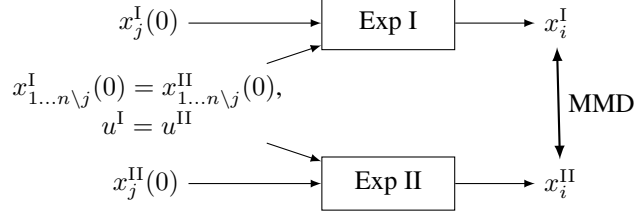


Figure 1: Experiment design for causal inference. We design two experiments, where all initial conditions and input trajectories are constant except for  $x_j(0)$ . If the resulting trajectory of  $x_i$  differs in both experiments, we have evidence that the change in  $x_j(0)$  caused this change.

distributions  $\mathbb{P}$  and  $\mathbb{Q}$  are equal based on samples drawn from these distributions. Let  $X$  and  $Y$  be samples drawn i.i.d. from  $\mathbb{P}$  and  $\mathbb{Q}$ , respectively. Further, let  $\mathcal{H}$  be a reproducing kernel Hilbert space [50], with canonical feature map  $\phi: \mathcal{X} \rightarrow \mathcal{H}$ . The MMD is defined as

$$\text{MMD}(\mathbb{P}, \mathbb{Q}) = \|\mathbb{E}_{X \sim \mathbb{P}}[\phi(X)] - \mathbb{E}_{Y \sim \mathbb{Q}}[\phi(Y)]\|_{\mathcal{H}}. \quad (3)$$

The feature map  $\phi$  can be expressed in terms of a kernel function  $k(\cdot, \cdot)$ , where  $k(x, y) = \langle \phi(x), \phi(y) \rangle_{\mathcal{H}}$ . If the kernel is characteristic, we have  $\text{MMD}(\mathbb{P}, \mathbb{Q}) = 0$  if, and only if,  $\mathbb{P} = \mathbb{Q}$  [16, 51]. In the remainder of the paper, we always assume a characteristic kernel (e.g., the Gaussian kernel).

In the following, we derive conditions that allow one to provably identify causal relations. We investigate three settings. First, we discuss the case where we can exactly steer the system to desired initial conditions (i.e.,  $\epsilon = 0$  in Definition 2). We then extend this to  $\epsilon \neq 0$ , which requires us to provide a stricter controllability definition. Finally, we show that for linear systems with additive Gaussian noise, the conditions stated by Kalman [19] are sufficient, and the identification is substantially easier.

#### 4.1 Exact Controllability

When considering control systems, data is highly correlated, and instead of stationary distributions, we are dealing with random processes as in (1). We design experiments of fixed length  $T$ . Thus, we have a sequence of  $T$  random variables, sampled at discrete intervals of fixed length, with joint distribution  $\mathbb{P}(x) = \mathbb{P}(x(0), \dots, x(T))$ . For these sequences, the MMD reads

$$\text{MMD}(x^I, x^{II}) = \|\mathbb{E}_{x^I \sim \mathbb{P}^I(x^I)}[\phi(x^I)] - \mathbb{E}_{x^{II} \sim \mathbb{P}^{II}(x^{II})}[\phi(x^{II})]\|_{\mathcal{H}}. \quad (4)$$

If we now design experiments (2), we can check the similarity of  $x_i$  trajectories using (4). An  $\text{MMD} > 0$  then suggests that trajectories are different, so we can conclude that there is a causal influence. However, the other direction is less straightforward: for a system (1), the MMD may be 0, even though variables are dependent, as can be seen in the following example:

**Example 1.** Assume a control system with  $x_1(t+1) = x_1(t)x_2(t)$  and  $x_2(t+1) = u(t)$ , and an input signal  $u(t)$  that is different from 0. If we choose  $x_1(0) = 0$ , the trajectory of  $x_1$  will, despite the fact that  $x_2$  clearly has a causal influence on  $x_1$ , always be 0 no matter the initial condition  $x_2(0)$ .

To address this, we define the concept of local non-causality:

**Definition 3** (Local non-causality). The state variable  $x_j$  does locally not cause  $x_i$  if  $x_i(t) = f_i(x_{1,\dots,n \setminus j}(0), x_j^I(0), u, v) = f_i(x_{1,\dots,n \setminus j}(0), x_j^{II}(0), u, v)$  given that  $x$  in  $\mathcal{X}_{\text{ind}}$  and  $u$  in  $\mathcal{U}_{\text{ind}}$ , where  $\mathcal{X}_{\text{ind}} \subseteq \mathcal{X}$  and  $\mathcal{U}_{\text{ind}} \subseteq \mathcal{U}$ .<sup>1</sup> Similarly,  $u_j$  does locally not cause  $x_i$  if  $x_i(t) = f_i(x(0), u_{1,\dots,m \setminus j}, u_j^I, v) = f_i(x(0), u_{1,\dots,m \setminus j}, u_j^{II}, v)$  given that  $x$  in  $\mathcal{X}_{\text{ind}}$  and  $u$  in  $\mathcal{U}_{\text{ind}}$ .

The non-causality becomes global if  $\mathcal{X}_{\text{ind}} = \mathcal{X}$  and  $\mathcal{U}_{\text{ind}} = \mathcal{U}$ . Similar notions have, under the term local independence, been discussed in [44, 1, 26]. We make the following assumption about the system (1) and the estimated model  $\hat{f}$ :

**Assumption 1.** For the system (1) it holds that either all non-causalities are global, or the local non-causalities are reflected by the estimated model  $\hat{f}$ . We say that local non-causalities are reflected

<sup>1</sup>In general, there may exist different  $\mathcal{X}_{\text{ind}}^{ij}$  for each combination of  $x_i$  and  $x_j$  (and likewise for  $\mathcal{U}_{\text{ind}}$ ). We can also cover this case. However, we omit it here to simplify notation.

by the model  $\hat{f}$  if the following holds: for experiments designed according to (2),  $\text{MMD}(\hat{x}_i^I, \hat{x}_i^{II} | \hat{f}) < \text{MMD}(\hat{x}_i^{III}, \hat{x}_i^{IV} | \hat{f})$  if  $\hat{x}_i^I$  and  $\hat{x}_i^{II}$  are inside  $\mathcal{X}_{\text{ind}}$  and the corresponding inputs are in  $\mathcal{U}_{\text{ind}}$ , while  $\hat{x}_i^{III}$  and  $\hat{x}_i^{IV}$  and their corresponding inputs take values outside these sets.  $\text{MMD}(\hat{x}_i^I, \hat{x}_i^{II} | \hat{f})$  denotes the MMD of simulated  $\hat{x}_i$  trajectories based on the model  $\hat{f}$ .

That is, we *do not* require that  $\hat{f}$  captures the causal structure. But we require that simulated trajectories in regions of local non-causality have a smaller MMD than trajectories in other regions.

**Example 1** (cont). Given Assumption 1, if we simulate experiments (2a) and compute the MMD for the resulting  $\hat{x}_1$ , the MMD will be lower if we choose  $\hat{x}_1(0)=0$  than for any other choice of  $\hat{x}_1(0)$ .

We now specify the experiment design. To avoid regions of local non-causality, we propose to maximize the MMD given the model estimate. Thus, for checking whether  $x_j$  causes  $x_i$ , we choose input trajectories of length  $T$  and initial conditions that solve

$$\max_{x^I(0), x^{II}(0), u^I, u^{II}} \text{MMD}(\hat{x}_i^I, \hat{x}_i^{II} | \hat{f}) \quad \text{subject to} \quad x_\ell^I(0) = x_\ell^{II}(0) \forall \ell \neq j \quad u_\ell^I(t) = u_\ell^{II}(t) \forall \ell, t. \quad (5a)$$

We will discuss how to handle this optimization problem in practice in Sec. 5.2. If we want to check whether  $u_j$  causes  $x_i$ , we choose input trajectories and initial conditions by solving

$$\max_{x^I(0), x^{II}(0), u^I, u^{II}} \text{MMD}(\hat{x}_i^I, \hat{x}_i^{II} | \hat{f}) \quad \text{subject to} \quad x_\ell^I(0) = x_\ell^{II}(0) \forall \ell \quad u_\ell^I(t) = u_\ell^{II}(t) \forall \ell \neq j, t. \quad (5b)$$

We can now state the main theorem:

**Theorem 1.** Assume a completely  $\epsilon$ -controllable system (1) with  $\epsilon = 0$  that fulfills Assumption 1. Let experiments be designed according to (5) for a fixed experiment length  $T < \infty$  and repeated infinitely often (i.e., we collect an infinite amount of realizations of two random processes). Then:  $\text{MMD}(x_i^I, x_i^{II}) = 0$  if, and only if, variables are non-causal according to Definition 1.

*Proof.* Let variables be non-causal. Then, the distribution of  $x_i$  in both experiments is equal. Thus,  $\text{MMD}(x_i^I, x_i^{II}) = 0$  follows from [17]. Now, assume  $\text{MMD}(x_i^I, x_i^{II}) = 0$ . This implies that the distribution of  $x_i$  is equal in both experiments [17]. By Assumption 1, the model reflects local non-causalities (if they exist). In that case, the optimization (5) ensures that we collect data outside of such regions. Thus, if distributions are equal, non-causality must be global as defined in Definition 1.  $\square$

**Remark 1.** The probability distribution can become independent of the initial conditions over time if the process is stable. Causal influences are then only visible during the transient. Thus, doing multiple short experiments is, in general, preferred over one long experiment. Also, in the case of non-ergodic systems, where time and spatial average are not the same, we only have a valid testing procedure if we do multiple runs of each experiment.

## 4.2 $\epsilon$ -Controllability

For a stochastic system as in (1), it is in general impossible to steer the system exactly to the initial conditions suggested by (5); i.e., we need to resort to controllability with  $\epsilon > 0$  (cf. Def. 2). But even in such cases, it is still possible to guarantee the consistency of the causality testing procedure. However, we need a stricter definition of controllability.

**Definition 4.** Let system (1) be controllable according to Definition 2, and consider some arbitrary, but fixed  $x_{\ell, \text{des}}^*$ . Then, the system (1) is said to be completely  $\epsilon$ -controllable in distribution if, for any  $x(0)$  and any  $x_{\text{des}}$  with  $x_{\ell, \text{des}} = x_{\ell, \text{des}}^*$ , there exists an input sequence  $u(0:t_f)$  such that  $x_\ell(t_f)$  always follows the same distribution; i.e.,  $P(x_\ell(t_f)) = P^*$  for some  $P^*$  that does not depend on  $x(0)$  or any component of  $x_{\text{des}}$  except  $x_{\ell, \text{des}} = x_{\ell, \text{des}}^*$ .

In other words, the definition states that, for any  $x(0)$ , we can generate input trajectories that guarantee that the fixed component  $x_{\ell, \text{des}}^*$  of  $x_{\text{des}}$  is matched in distribution. Linear systems with additive Gaussian noise that are controllable following [19] are also controllable in the sense of Definition 4, as we show in the supplementary material. We further need to assume that connected regions without local non-causalities have a radius of at least  $\sqrt{\epsilon}$  to be able to steer the system to those regions.

**Assumption 2.** For all connected subsets  $\mathcal{X}_{i, \text{con}}$  of  $\mathcal{X} \setminus \mathcal{X}_{\text{ind}}$ , we assume that for all  $x \in \mathcal{X}_{i, \text{con}}$ , there exists an  $n$ -dimensional sphere with radius at least  $\sqrt{\epsilon}$  that includes  $x$  and that is inside  $\mathcal{X}_{i, \text{con}}$ .

This assumption is needed to exclude corner cases in which the causal influence only exists in single points of the state and input space. In such cases, the probability of successfully steering the system to those points is 0. However, considering the variables as non-causal may then anyway be reasonable. Equipped with these two assumptions, we can now state:

**Corollary 1.** *Assume a system (1) that is completely  $\epsilon$ -controllable in distribution according to Definition 4 and fulfills Assumptions 1 and 2. Let experiments be designed as in (5) for a fixed experiment length  $T < \infty$ , trajectories that steer the system to the initial conditions of the experiments be chosen such that  $P(x_\ell^I(0)) = P(x_\ell^{II}(0)) \forall \ell \neq j$ , and experiments be repeated infinitely often. Then:  $\text{MMD}(x_i^I, x_i^{II}) = 0$  if, and only if, variables are non-causal according to Definition (1).*

*Proof.* Let variables be non-causal. Then, we have  $P(x_\ell^I(0)) = P(x_\ell^{II}(0)) \forall \ell \neq j$ , thus, also the distribution of the obtained  $x_i$  trajectories is equal and we have  $\text{MMD}(x_i^I, x_i^{II}) = 0$  [17]. Now, assume  $\text{MMD}(x_i^I, x_i^{II}) = 0$ . This implies that the distribution of  $x_i$  is equal in both experiments [17]. By Assumption 1, existing local non-causalities are reflected by the model and thus, (5) will suggest experiments outside of such regions. Assumption 2 ensures that we can steer the system to those regions. Thus, if distributions are equal, non-causality must be global as in Definition 1.  $\square$

### 4.3 Linear Systems

Local non-causality as in Definition 3 is a nonlinear phenomenon. If we assume (1) to be linear time-invariant (LTI) with Gaussian noise  $v(t)$ , we can reveal the true causal structure without the optimization procedure (5), making this case substantially easier. For an LTI system, (1) reads

$$x(t) = A^t x(0) + \sum_{i=0}^{t-1} A^i (Bu(t-1-i) + v(t-1-i)), \quad (6)$$

with state transition matrix  $A \in \mathbb{R}^{n \times n}$ , input matrix  $B \in \mathbb{R}^{n \times m}$ , and  $v(t) \sim \mathcal{N}(0, \Sigma)$ . The system (6) is controllable as per Definition 4 if it satisfies the classical controllability condition from [19], i.e., if the matrix  $\begin{pmatrix} B & AB & \dots & A^{n-1}B \end{pmatrix}$  has full row rank, as we show in Lemma 1 in the appendix. We can then state the following theorem, whose proof is provided in the supplementary material:

**Theorem 2.** *Assume an LTI system (6), whose deterministic part is controllable in the sense of Kalman. Let experiments be designed as in (2a) and (2b), respectively. Then:  $\text{MMD}(x_i^I, x_i^{II}) = 0$  if, and only if, the variables are non-causal as per Definition 1.*

## 5 Implementation

The results in Sec. 4 show that we are able to detect whether the variables  $x_j$  or  $u_j$  have a causal influence on  $x_i$ . In practical implementations, two challenges remain: first, we can only collect a finite amount of data and, thus, need an approximation of the MMD and a test statistic. Second, we may not be able to obtain a global solution to (5).

### 5.1 Test with Finite Samples

Given  $m$  samples of  $X$  and  $Y$  (with  $m < \infty$ ), the squared MMD can be approximated as [17]

$$\text{MMD}^2(X, Y) \approx \frac{1}{m(m-1)} \sum_{i \neq j}^m (k(x_i, x_j) + k(y_i, y_j) - k(x_i, y_j) - k(x_j, y_i)). \quad (7)$$

For a finite sample size  $m$ , the MMD will, in general, not equal 0 if distributions are equal. Obtaining a test statistic for the MMD valid for control systems (1) is non-trivial. Here, we exploit that we can obtain an estimate of the model and its uncertainty. We estimate a model  $\hat{f}_{i,\text{ind}}$  that assumes  $x_i$  and  $x_j$  respectively  $u_j$  are non-causal (i.e., we do not use the data  $x_j$  respectively  $u_j$  when estimating  $\hat{f}_{i,\text{ind}}$ ). We propose to use this model to decide whether to accept the null hypothesis of  $x_i$  and  $x_j$  respectively  $u_j$  being non-causal and, thus, update the current model estimate  $\hat{f}$ :

$$\hat{f}_i = \hat{f}_{i,\text{ind}} : \Leftrightarrow \text{MMD}^2(x_i^I, x_i^{II}) < \mathbb{E}[\text{MMD}^2(\hat{x}_i^I, \hat{x}_i^{II}) | \hat{f}_{i,\text{ind}}] + \nu \sqrt{\text{Var}[\text{MMD}^2(\hat{x}_i^I, \hat{x}_i^{II}) | \hat{f}_{i,\text{ind}}]}. \quad (8)$$

Algorithm 1: Pseudocode of the proposed framework.

```

1: Excite system with input signal, collect data
2: Obtain  $\hat{f}$  through black-box system identification
3: for  $x_j$  in  $x$  do
4:    $x_{\text{test}} = [x_1, \dots, x_n]$ 
5:   for  $x_\ell$  in  $x_{\text{test}}$  do
6:     Run (5a) until  $\mathbb{E}[\text{MMD}^2(\hat{x}_\ell^I, \hat{x}_\ell^{II}|\hat{f})] > \delta_1$ 
7:     Run causal experiments, collect data
8:     for  $x_i$  in  $x_{\text{test}}$  do
9:       if  $\mathbb{E}[\text{MMD}^2(\hat{x}_i^I, \hat{x}_i^{II}|\hat{f})] > \delta_2$  then
10:        Obtain  $\hat{f}_{i,\text{ind}}$ 
11:        Obtain test statistic via Monte Carlo simulations
12:        if (8) holds then
13:           $\hat{f}_i = \hat{f}_{i,\text{ind}}$ 
14:        Delete  $x_i$  from  $x_{\text{test}}$ 

```

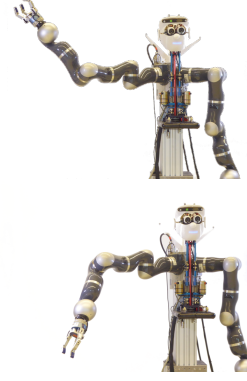


Figure 2: The robotic system showing initial postures for two experiments.

Expected value and variance in (8) can be estimated through Monte Carlo simulations. For these simulations, we use the true initial conditions  $x^I(0)$  and  $x^{II}(0)$ , that way accounting for uncertainty due to unequal initial conditions between experiments. The significance level of the test can be adjusted through  $\nu$  using Chebyshev’s inequality [6].

## 5.2 Experiment Design

The framework for testing causality between state variables is summarized in Alg. 1 (and works analogously for inputs)<sup>2</sup>. After having obtained an initial model (ll. 1-2), we run (5a) to find initial conditions and input trajectories for testing non-causality of one specific combination of  $x_\ell$  and  $x_j$  (l. 6). The optimization in (5a) may be arbitrarily complex or even intractable, depending on the chosen model class. However, finding a global optimum of (5a) is not necessary. The goal of the optimization procedure is to avoid regions of local non-causality. We thus optimize (5a) until it is above a threshold  $\delta_1$  to be confident that we are not in a region of local non-causality. In practical applications, we can often already achieve this through a reasonable initialization of the optimization problem, i.e., by choosing initial conditions for  $x_j$  as far apart as possible. We then run the designed experiment and collect the data (l. 7). Ideally, we would like to use data from this single experiment to test for causal influence of  $x_j$  on all other state components. Thus, we check for which  $x_i$  the experiment yields an expected MMD that is higher than a second threshold  $\delta_2$  and do the hypothesis test for all of those (ll. 9-13).

## 6 Robot Experiments

We evaluate the framework by identifying the causal structure of one arm of the robot in Fig. 2. We consider kinematic control of the robot; that is, we can command desired angular velocities to the joints, which are then tracked by low-level controllers (taking care, i.a., of the robot dynamics). As measurements, we receive the joint angles. The goal of the causal identification is to learn which joints influence each other, and which joints are influenced by which inputs. We consider four joints of the robot arm in the following experiments. From the robot arm’s design, we know its kinematic structure, which is described by  $\dot{\phi}_i = \tau_i$  for each joint, where  $\phi_i$  denotes the angle of joint  $i$  and  $\tau_i$  the applied motor torque. That is, we expect each joint velocity  $\dot{\phi}_i$  to depend only on the local input  $\tau_i$  and not other variables. While the dynamics are approximately linear, we do not rely on this information and are thus in the setting discussed in Sec. 4.2. In the following, we will investigate if our proposed causal identification can reveal this structure automatically. For this, we describe the setting and discuss the results, while we defer implementation details to the supplementary material.

Following Alg. 1, we start by identifying a model  $\hat{f}$ . As expected, the initial model suggests that all joints are linked to each other and to all inputs owing to spurious correlations. We then design

<sup>2</sup>An implementation is available at [https://github.com/baumannndominik/identifying\\_causal\\_structure](https://github.com/baumannndominik/identifying_causal_structure).

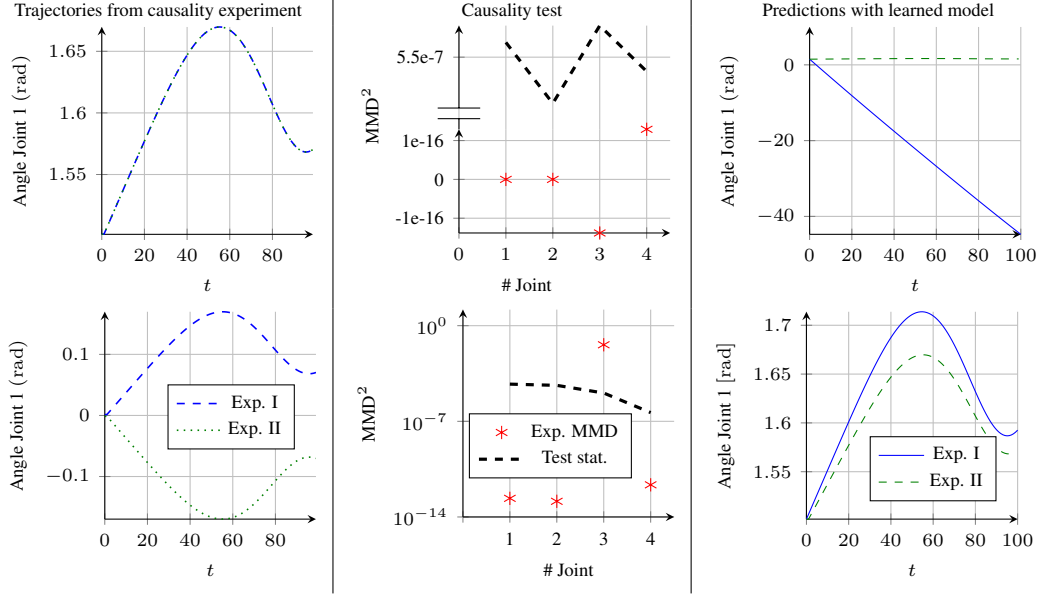


Figure 3: Causality tests and model evaluation. *Plots on the left show example trajectories of two experiments, in the middle the experimental MMD and the test threshold for joint 3, and on the right predictions based on the initial model and on the refined model after the causal identification.*

experiments for causality testing, example trajectories of such experiments are shown in Fig. 3 (left). The empirical squared MMD of the resulting trajectories is compared with the test statistic. The trajectories in Fig. 3 (left) already suggest that the experiments are in line with the kinematic model: while the two trajectories of joint 1 for different initial conditions of joint 3 are essentially equal (blue dashed and green dotted lines overlap), the trajectories of joint 3 for different choices of the third input are fundamentally different. This is also revealed through the proposed causality test. The middle plots of Fig. 3 show the empirical squared MMD (left-hand side of inequality (8)) and the test threshold (right-hand side of (8)) for the experiments that were conducted to test the influence of the initial conditions of the third joint (top) and of the third input signal (bottom) on all joints. As can be seen, the causal identification reveals that the third joint does not influence any other joint, and the third input only affects the third joint. Note that the trajectories of the third joint are obviously different when we choose different initial conditions for the third joint. However, since this is expected, we subtract the initial condition in this case to investigate whether the movement starting from these distinct initial conditions differs. The remaining experiments (results are contained in the supplementary material) yield similar results. In summary, the causal identification successfully reveals the expected causal structure.

To investigate the generalization capability, we compare predictions of the model  $\hat{f}_{\text{init}}$  obtained from the initial system identification and the model  $\hat{f}_{\text{caus}}$  that was learned after revealing the causal structure. In both cases, we use the same training data to estimate the model parameters. However, for  $\hat{f}_{\text{caus}}$ , we leverage the obtained knowledge of the causal structure when estimating parameters, while for  $\hat{f}_{\text{init}}$  we do not take any prior knowledge into account. As test data, we use an experiment that was conducted to investigate the influence of the initial condition of joint 3 on the other joints and let both models predict the trajectory of joint 1. For this experiment, the initial angle of joint 3 is close to its maximum value, a case that is not contained in the training data. As can be seen in Fig. 3 (right), the predictions of  $\hat{f}_{\text{caus}}$  (blue) are very close to the true data (green, dashed), i.e., the model can generalize well, while the predictions of  $\hat{f}_{\text{init}}$  deviate significantly.

## 7 Conclusion

We presented a method that identifies the causal structure of dynamical control systems by conducting experiments and analyzing the generated data with the MMD. It differs from prior approaches to



causal inference in that it uses a controllability notion that is suitable to design experiments for control systems. We evaluated the method on a real-world robotic system. Our algorithm successfully identified the underlying causal structure, which in turn allowed us to learn a model that accurately generalizes to previously unseen states. For ease of trying out our method, we also provide a synthetic example with code in the supplementary material.

## Broader Impact

In this paper, we propose a method for learning more reliable models for dynamical control systems. In particular, we enable control systems to learn about their causal structure, which results in better generalization capabilities. The method can thus help in improving the performance of autonomous systems when letting them explore their environment. This work can thus be seen as a contribution towards building more reliable and trustworthy autonomous systems, such as mobile robots, with many envisioned use cases in the real world, which also includes issues of dual-use.

## Acknowledgments and Disclosure of Funding

The authors would like to thank Manuel Wüthrich and Alonso Marco Valle for insightful discussions, Steve Heim for valuable feedback, and Vincent Berenz for support with the robot experiments. This work was supported in part by the German Research Foundation within the SPP 1914 (grant TR 1433/1-1), the Cyber Valley Initiative, and the Max Planck Society.

## References

- [1] Odd O Aalen. Dynamic modelling and causality. *Scandinavian Actuarial Journal*, 1987(3-4):177–190, 1987.
- [2] Hirotogu Akaike. Information theory and an extension of the maximum likelihood principle. In *International Symposium on Information Theory*, pages 267–281, 1973.
- [3] Brian DO Anderson and John B Moore. *Optimal Control: Linear Quadratic Methods*. Courier Corporation, 2007.
- [4] Agamirza E Bashirov and Kerim R Kerimov. On controllability conception for stochastic systems. *SIAM Journal on Control and Optimization*, 35(2):384–398, 1997.
- [5] Stefano Boccaletti, Vito Latora, Yamir Moreno, Martin Chavez, and Dong-Uk Hwang. Complex networks: Structure and dynamics. *Physics Reports*, 424(4-5):175–308, 2006.
- [6] Pafnutii Lvovich Chebyshev. Sur les valeurs limites des intégrales. *Journal de Mathématiques Pures et Appliquées*, 2(19):157–160, 1874.
- [7] Zhitang Chen, Kun Zhang, Laiwan Chan, and Bernhard Schölkopf. Causal discovery via reproducing kernel Hilbert space embeddings. *Neural Computation*, 26(7):1484–1517, 2014.
- [8] Tianjiao Chu and Clark Glymour. Search for additive nonlinear time series causal models. *Journal of Machine Learning Research*, 9(May):967–991, 2008.
- [9] Kacper Chwialkowski and Arthur Gretton. A kernel independence test for random processes. In *International Conference on Machine Learning*, pages 1422–1430, 2014.
- [10] Kacper Chwialkowski, Dino Sejdinovic, and Arthur Gretton. A wild bootstrap for degenerate kernel tests. In *Advances in Neural Information Processing Systems*, pages 3608–3616, 2014.
- [11] Selva Demiralp and Kevin D Hoover. Searching for the causal structure of a vector autoregression. *Oxford Bulletin of Economics and Statistics*, 65:745–767, 2003.
- [12] Michael Eichler. Graphical Gaussian modelling of multivariate time series with latent variables. In *International Conference on Artificial Intelligence and Statistics*, pages 193–200, 2010.
- [13] Michael Eichler. Causal inference in time series analysis. In Carlo Berzuini, Philip Dawid, and Luisa Bernardinell, editors, *Causality: Statistical Perspectives and Applications*, chapter 22, pages 327–354. John Wiley & Sons, Ltd, 2012.

- [14] Doris Entner and Patrik O Hoyer. On causal discovery from time series data using FCI. *Probabilistic Graphical Models*, pages 121–128, 2010.
- [15] Karl J Friston, Lee Harrison, and Will Penny. Dynamic causal modelling. *Neuroimage*, 19(4):1273–1302, 2003.
- [16] Kenji Fukumizu, Arthur Gretton, Xiaohai Sun, and Bernhard Schölkopf. Kernel measures of conditional dependence. In *Advances in Neural Information Processing Systems*, pages 489–496, 2008.
- [17] Arthur Gretton, Karsten M Borgwardt, Malte J Rasch, Bernhard Schölkopf, and Alexander Smola. A kernel two-sample test. *Journal of Machine Learning Research*, 13(Mar):723–773, 2012.
- [18] Joao P Hespanha. *Linear Systems Theory*. Princeton University Press, 2018.
- [19] Rudolf Emil Kalman. Contributions to the theory of optimal control. *Boletín de la Sociedad Matemática Mexicana*, 5(2):102–119, 1960.
- [20] Fabien Lauer and Gérard Bloch. *Hybrid System Identification: Theory and Algorithms for Learning Switching Models*. Springer, 2018.
- [21] Hui Liu, Jun-An Lu, Jinhu Lü, and David J Hill. Structure identification of uncertain general complex dynamical networks with time delay. *Automatica*, 45(8):1799–1807, 2009.
- [22] Lennart Ljung. *System Identification: Theory for the User*. Prentice Hall PTR, 1999.
- [23] David Lopez-Paz, Krikamol Muandet, Bernhard Schölkopf, and Ilya Tolstikhin. Towards a learning theory of cause-effect inference. In *International Conference on Machine Learning*, pages 1452–1461, 2015.
- [24] Daniel Malinsky and Peter Spirtes. Causal structure learning from multivariate time series in settings with unmeasured confounding. In *ACM SIGKDD Workshop on Causal Discovery*, pages 23–47, 2018.
- [25] Donatello Materassi and Giacomo Innocenti. Topological identification in networks of dynamical systems. *IEEE Transactions on Automatic Control*, 55(8):1860–1871, 2010.
- [26] Søren Wengel Mogensen and Niels Richard Hansen. Markov equivalence of marginalized local independence graphs. *The Annals of Statistics*, 48(1):539–559, 2020.
- [27] Alessio Moneta, Nadine Chlaß, Doris Entner, and Patrik Hoyer. Causal search in structural vector autoregressive models. In *NIPS Mini-Symposium on Causality in Time Series*, pages 95–114, 2011.
- [28] Joris M. Mooij, Dominik Janzing, and Bernhard Schölkopf. From ordinary differential equations to structural causal models: The deterministic case. In *Conference on Uncertainty in Artificial Intelligence*, page 440–448, 2013.
- [29] Joris M Mooij, Jonas Peters, Dominik Janzing, Jakob Zscheischler, and Bernhard Schölkopf. Distinguishing cause from effect using observational data: methods and benchmarks. *The Journal of Machine Learning Research*, 17(1):1103–1204, 2016.
- [30] Duy Nguyen-Tuong and Jan Peters. Model learning for robot control: A survey. *Cognitive Processing*, 12(4):319–340, 2011.
- [31] Gabriele Pannocchia, Nabil Laachi, and James B Rawlings. A candidate to replace PID control: SISO-constrained LQ control. *AIChE Journal*, 51(4):1178–1189, 2005.
- [32] Grigorios A Pavliotis. *Stochastic Processes and Applications: Diffusion Processes, the Fokker-Planck and Langevin Equations*. Springer, 2014.
- [33] Judea Pearl. Causal diagrams for empirical research. *Biometrika*, 82(4):669–688, 1995.
- [34] Judea Pearl and Dana Mackenzie. *The Book of Why: The New Science of Cause and Effect*. Basic Books, 2018.
- [35] Jonas Peters, Stefan Bauer, and Niklas Pfister. Causal models for dynamical systems. *arXiv preprint arXiv:2001.06208*, 2020.
- [36] Jonas Peters, Dominik Janzing, and Bernhard Schölkopf. Causal inference on time series using restricted structural equation models. In *Advances in Neural Information Processing Systems*, pages 154–162, 2013.
- [37] Jonas Peters, Dominik Janzing, and Bernhard Schölkopf. *Elements of Causal Inference: Foundations and Learning Algorithms*. MIT Press, 2017.

- [38] Christopher J Quinn, Todd P Coleman, Negar Kiyavash, and Nicholas G Hatsopoulos. Estimating the directed information to infer causal relationships in ensemble neural spike train recordings. *Journal of Computational Neuroscience*, 30(1):17–44, 2011.
- [39] Jacob Roll, Alberto Bemporad, and Lennart Ljung. Identification of piecewise affine systems via mixed-integer programming. *Automatica*, 40(1):37–50, 2004.
- [40] Paul K. Rubenstein, Stephan Bongers, Bernhard Schölkopf, and Joris M. Mooij. From deterministic ODEs to dynamic structural causal models. In *Conference on Uncertainty in Artificial Intelligence*, 2018.
- [41] Bernhard Schölkopf. Causality for machine learning. *arXiv preprint arXiv:1911.10500*, 2019.
- [42] Johan Schoukens and Lennart Ljung. Nonlinear system identification: A user-oriented road map. *IEEE Control Systems Magazine*, 39(6):28–99, 2019.
- [43] Gideon Schwarz. Estimating the dimension of a model. *The Annals of Statistics*, 6(2):461–464, 1978.
- [44] Tore Schweder. Composable Markov processes. *Journal of Applied Probability*, 7(2):400–410, 1970.
- [45] Shahin Shahrampour and Victor M Preciado. Topology identification of directed dynamical networks via power spectral analysis. *IEEE Transactions on Automatic Control*, 60(8):2260–2265, 2014.
- [46] Karthikeyan Shanmugam, Murat Kocaoglu, Alexandros G Dimakis, and Sriram Vishwanath. Learning causal graphs with small interventions. In *Advances in Neural Information Processing Systems*, pages 3195–3203, 2015.
- [47] Max Simchowitz, Horia Mania, Stephen Tu, Michael I. Jordan, and Benjamin Recht. Learning without mixing: Towards a sharp analysis of linear system identification. In *Conference on Learning Theory*, pages 439–473, 2018.
- [48] Alexander Sokol and Niels Richard Hansen. Causal interpretation of stochastic differential equations. *Electronic Journal of Probability*, 19(100):1–24, 2014.
- [49] Peter Spirtes, Clark N Glymour, Richard Scheines, David Heckerman, Christopher Meek, Gregory Cooper, and Thomas Richardson. *Causation, Prediction, and Search*. MIT Press, 2000.
- [50] Bharath K Sriperumbudur, Arthur Gretton, Kenji Fukumizu, Bernhard Schölkopf, and Gert RG Lanckriet. Hilbert space embeddings and metrics on probability measures. *Journal of Machine Learning Research*, 11(Apr):1517–1561, 2010.
- [51] Ingo Steinwart. On the influence of the kernel on the consistency of support vector machines. *Journal of Machine Learning Research*, 2(Nov):67–93, 2001.
- [52] Klaas Enno Stephan, Will D Penny, Rosalyn J Moran, Hanneke EM den Ouden, Jean Daunizeau, and Karl J Friston. Ten simple rules for dynamic causal modeling. *Neuroimage*, 49(4):3099–3109, 2010.
- [53] Yoshifumi Sunahara, Teruo Kabeuchi, Yoshiharu Asada, Shin Ichi Aihara, and Kiyotaka Kishino. On stochastic controllability for nonlinear systems. *IEEE Transactions on Automatic Control*, 19(1):49–54, 1974.
- [54] Paul MJ van den Hof, Arne Dankers, Peter SC Heuberger, and Xavier Bombois. Identification of dynamic models in complex networks with prediction error methods—basic methods for consistent module estimates. *Automatica*, 49(10):2994–3006, 2013.
- [55] Halbert White and Xun Lu. Granger causality and dynamic structural systems. *Journal of Financial Econometrics*, 8(2):193–243, 2010.
- [56] Karren D Yang, Abigail Katcoff, and Caroline Uhler. Characterizing and learning equivalence classes of causal DAGs under interventions. *arXiv preprint arXiv:1802.06310*, 2018.
- [57] Dongchuan Yu. Estimating the topology of complex dynamical networks by steady state control: Generality and limitation. *Automatica*, 46(12):2035–2040, 2010.

## A Proof of Theorem 2

An LTI system with Gaussian noise follows a normal distribution, whose mean is given by

$$x(t) = A^t x(0) + \sum_{i=0}^{t-1} A^i B u(t-1-i) \quad (9)$$

and whose variance only depends on time and the variance of  $v(t)$  [32, Sec. 3.7], which we assume to be constant. For such systems, we will first show that if (9) obeys the controllability conditions stated by Kalman, the system is also controllable according to Definitions 2 and 4.

**Lemma 1.** *The system (6) is completely  $\epsilon$ -controllable in distribution if the deterministic part obeys the controllability condition stated in [19].*

*Proof.* The expected value (9) represents the deterministic part of the system. Thus, according to [19], we can steer (9) to any point in the state space. The variance only depends on the number of time steps. Since we can steer the linear system to any point  $x_{\text{des}}$  in the state space in any amount of time steps, we can ensure that all trajectories are of equal length. Then, the distribution of the final state has mean  $x_{\text{des}}$  and a variance that depends on the chosen number of time steps. The probability of  $\|x_i - x_{i,\text{des}}\|_2^2$  being larger than  $\epsilon$  is given by the cumulative distribution function of the normal distribution.  $\square$

We can now prove Theorem 2. Since the variance of (6) solely depends on the number of time steps, which is equal for all experiments, distributions can only be different because of their means. We start with experiments that are designed according to (2a). In this case, for distributions to be equal, and, thus, for variables to be non-causal, we need

$$e_i \left( A^t x^I(0) + \sum_{i=0}^{t-1} A^i (B u(t-1-i)) \right) = e_i \left( A^t x^{\text{II}}(0) + \sum_{i=0}^{t-1} A^i (B u(t-1-i)) \right),$$

where  $e_i \in \mathbb{R}^n$  is the unit vector (i.e., a vector with zeros and a single 1 at the  $i$ th entry). Since input trajectories are equal, this boils down to

$$e_i A^t x^I(0) = e_i A^t x^{\text{II}}(0).$$

Essentially this means that the component  $ij$  of  $A^t$  needs to be 0. This is clearly the case, if there is no influence of  $x_i$  on  $x_j$ , i.e., in case variables are non-causal, we have  $\text{MMD} = 0$ . The event of component  $ij$  of the matrix exponential being 0 by chance, even though  $x_j$  has a causal influence on  $x_i$ , has probability 0. Thus, we have that variables are non-causal if  $\text{MMD} = 0$ .

For experiments that are designed according to (2b), initial states are equal and, in case variables are non-causal, we have

$$e_i \sum_{i=0}^{t-1} A^i (B u^I(t-1-i)) = e_i \sum_{i=0}^{t-1} A^i (B u^{\text{II}}(t-1-i)).$$

Similar as before, we have equal distributions and, thus,  $\text{MMD} = 0$  if entries in the  $A$  and  $B$  matrices relating  $x_i$  and  $u_j$  are 0, i.e., if there is no causal influence. The other direction holds since the event of the relevant entries of  $A$  and  $B$  being 0 by chance has probability 0.

## B Experiment Details and Further Results

We first provide implementation details for the experiments presented in Sec. 6. The initial model estimate is obtained by exciting the system with a chirp signal for 30 s and using the generated data to learn a linear state-space model (cf. (6)) with least squares. The obtained matrices are

$$A_{\text{init}} \approx \begin{pmatrix} 0.868 & -0.132 & 0.754 & -0.491 \\ -0.132 & 0.868 & 0.754 & -0.491 \\ -0.132 & -0.132 & 1.754 & -0.491 \\ -0.134 & -0.134 & 0.76 & 0.508 \end{pmatrix} \quad B_{\text{init}} \approx \begin{pmatrix} 0.075 & -0.056 & -0.031 & 0.022 \\ 0.074 & -0.055 & -0.031 & 0.022 \\ 0.074 & -0.056 & -0.03 & 0.022 \\ 0.075 & -0.056 & -0.032 & 0.022 \end{pmatrix}$$

Initial conditions and input trajectories for the causality testing experiments are obtained through reasonable guesses, as discussed in Sec. 5.2. The found initial conditions and input trajectories yield expected MMDs that are orders of magnitude above the system's noise level for all joints. Thus, we do not need to fix variables  $\delta_1$  and  $\delta_2$  and, overall, only need 8 experiments to identify the causal structure. For each experiment, we design input trajectories of 100 time steps, repeat the experiment 10 times, and use collected data from all experiments for

Table 1: Results of the causal structure identification for a robot arm: Causal influences of joints on each other.

Joint → Joint	Experimental MMD	Test statistic
$x_1 \rightarrow x_1$	0	$1.65 \times 10^{-4}$
$x_1 \rightarrow x_2$	0	$1.79 \times 10^{-4}$
$x_1 \rightarrow x_3$	0	$2.39 \times 10^{-4}$
$x_1 \rightarrow x_4$	$2.43 \times 10^{-13}$	$1.61 \times 10^{-4}$
$x_2 \rightarrow x_1$	0	$5.6 \times 10^{-7}$
$x_2 \rightarrow x_2$	$-2.8 \times 10^{-18}$	$4.58 \times 10^{-7}$
$x_2 \rightarrow x_3$	0	$3.56 \times 10^{-7}$
$x_2 \rightarrow x_4$	$1.82 \times 10^{-13}$	$6.91 \times 10^{-7}$
$x_3 \rightarrow x_1$	0	$5.81 \times 10^{-7}$
$x_3 \rightarrow x_2$	0	$4.54 \times 10^{-7}$
$x_3 \rightarrow x_3$	$-1.38 \times 10^{-18}$	$6.16 \times 10^{-7}$
$x_3 \rightarrow x_4$	$1.29 \times 10^{-16}$	$5.2 \times 10^{-7}$
$x_4 \rightarrow x_1$	0	$4.99 \times 10^{-7}$
$x_4 \rightarrow x_2$	0	$4.66 \times 10^{-7}$
$x_4 \rightarrow x_3$	$9.63 \times 10^{-15}$	$5.8 \times 10^{-7}$
$x_4 \rightarrow x_4$	$-5.44 \times 10^{-15}$	$5.8 \times 10^{-7}$

hypothesis testing. The empirical squared MMD is computed with a Gaussian kernel with a lengthscale of 1. While the squared MMD is always positive, the empirical approximation (7) can become negative since it is an unbiased estimate. For the test statistic (8), we estimate the variance using 100 Monte Carlo simulations and obtain the expected value through a noiseless simulation. We use  $\nu = 1$ , but as we will see in the results, the empirical MMD is in all cases orders of magnitude below or above the threshold. Thus, also more conservative choices of  $\nu$  would yield the same outcome.

In Tables 1 and 2, we present the results of all causality testing experiments conducted on the robotic platform shown in Fig. 2. As for the results discussed in Sec. 6, we always have a clear decision on whether to accept or reject the null hypothesis: The MMD found in experiments is always orders of magnitude larger or smaller than the test statistic. Also here, we find that all joints can be moved independently of each other and are affected by exactly one input. When exploiting the revealed causal structure for identifying the system matrices, we obtain

$$A_{\text{caus}} = \begin{pmatrix} 1 & 0 & 0 & 0 \\ 0 & 1 & 0 & 0 \\ 0 & 0 & 1 & 0 \\ 0 & 0 & 0 & 1 \end{pmatrix} \quad B_{\text{caus}} \approx \begin{pmatrix} 0.013 & 0 & 0 & 0 \\ 0 & 0.007 & 0 & 0 \\ 0 & 0 & 0.01 & 0 \\ 0 & 0 & 0 & 0.01 \end{pmatrix}.$$

## C Synthetic Example and Code

In this section, we present a synthetic, linear example<sup>3</sup>. We consider an LTI system as in (6), with

$$A = \begin{pmatrix} 0.9 & -0.75 & 1.2 \\ 0 & 0.9 & -1.1 \\ 0 & 0 & 0.7 \end{pmatrix} \quad B = \begin{pmatrix} 0.03 & 0 & 0 \\ 0 & 0.06 & 0 \\ 0.07 & 0 & 0.05 \end{pmatrix}$$

and Gaussian noise with standard deviation  $1 \times 10^{-4}$ . For this example, we apply Alg. 1 (without the need for the optimization procedure since the example is linear) and can infer the causal structure implied by the state-space equation. In particular, the causal analysis reveals that  $x_1$  does not cause  $x_2$  nor  $x_3$ ,  $x_2$  does not cause  $x_3$ , and  $u_2$  does not cause  $x_3$ .

We here again want to stress the importance of an appropriate notion of controllability. Also in this example, it is not possible to *set* state variables to particular values. Thus, before starting a causality testing experiment, we always *steer* the system to the initial conditions required for that experiment. For this, we employ an approach to set-point tracking that has, for instance, been discussed in [31]. Given a desired state  $x_{\text{des}}$ , we seek a feedback control law of the form  $u = Mx_{\text{des}} + Fx$ , i.e., a control law that depends both on the desired state and the

<sup>3</sup>Code available at [https://github.com/baumannndominik/identifying\\_causal\\_structure](https://github.com/baumannndominik/identifying_causal_structure).

Table 2: Results of the causal structure identification for a robot arm: Causal influences of inputs on joints.

Input → Joint	Experimental MMD	Test statistic
$u_1 \rightarrow x_1$	0.04	$1.18 \times 10^{-5}$
$u_1 \rightarrow x_2$	0	$5.38 \times 10^{-7}$
$u_1 \rightarrow x_3$	0	$6.51 \times 10^{-7}$
$u_1 \rightarrow x_4$	0	$4.47 \times 10^{-7}$
$u_2 \rightarrow x_1$	0	$5.09 \times 10^{-5}$
$u_2 \rightarrow x_2$	0.04	$1.15 \times 10^{-5}$
$u_2 \rightarrow x_3$	$3.51 \times 10^{-14}$	$5.95 \times 10^{-7}$
$u_2 \rightarrow x_4$	$3.51 \times 10^{-14}$	$4.67 \times 10^{-7}$
$u_3 \rightarrow x_1$	$2.31 \times 10^{-13}$	$5.26 \times 10^{-5}$
$u_3 \rightarrow x_2$	$1.4 \times 10^{-13}$	$4.28 \times 10^{-5}$
$u_3 \rightarrow x_3$	0.04	$1.18 \times 10^{-5}$
$u_3 \rightarrow x_4$	$2.25 \times 10^{-12}$	$4.36 \times 10^{-7}$
$u_4 \rightarrow x_1$	0	$4.47 \times 10^{-5}$
$u_4 \rightarrow x_2$	0	$5.11 \times 10^{-5}$
$u_4 \rightarrow x_3$	0	$5.69 \times 10^{-7}$
$u_4 \rightarrow x_4$	0.04	$6.58 \times 10^{-4}$

current state. We obtain the gain matrix  $F$  using standard methods from linear optimal control [3], in particular, the linear quadratic regulator (LQR). Thus, we can rewrite the incremental dynamics of the system as

$$x(t+1) = A_{\text{cl}}x(t) + BMx_{\text{des}} + v(t), \quad (10)$$

where  $A_{\text{cl}} = A + BF$ . We now choose the feedforward term  $M$  such that the reference is matched in stationarity, i.e., we want to achieve

$$x = (I - A_{\text{cl}})^{-1}BMx_{\text{des}}. \quad (11)$$

Thus, we need

$$M = ((I - A_{\text{cl}})^{-1}B)^{-1} \quad (12)$$

to track the reference point. To compute  $M$ , we use the matrices  $\hat{A}$  and  $\hat{B}$  of the estimated model  $\hat{f}$ . We start the experiment once  $\|x(t) - x_{\text{des}}\|_2 < 0.01$ .